

000  
001  
002  
003  
004  
005  
006  
007  
008  
009  
010  
011  
012  
013  
014  
015  
016  
017  
018  
019  
020  
021  
022  
023  
024  
025  
026  
027  
028  
029  
030  
031  
032  
033  
034  
035  
036  
037  
038  
039  
040  
041  
042  
043  
044  
045  
046  
047  
048  
049  
050  
051  
052  
053

---

# Persistent Homology of Collaboration Networks

---

**C. J. Carstens**

School of Mathematical and Geospatial Sciences  
RMIT University  
Melbourne 3001, Australia  
corriejacobien.carstens@rmit.edu.au

**K. J. Horadam**

School of Mathematical and Geospatial Sciences  
RMIT University  
Melbourne 3001, Australia  
kathy.horadam@rmit.edu.au

## Abstract

We apply persistent homology to four collaboration networks. We show that the intervals for the zeroth and first Betti numbers correspond to tangible features of the structure of these networks. Finally, we use persistent homology to distinguish collaboration networks from similar random networks.

## 1 Introduction

Connections in social networks have different strengths. Some people in a social network are close friends or family, others are colleagues and yet others are merely acquaintances. These differences carry interesting information about the structure of a social network. As argued by Granovetter in his famous paper [1], the ties of different strength also perform different functions. Strong ties are found in clusters or groups, and the weak ties connect these groups.

We may use weighted networks to model a social network with different strengths. Weighted networks are often transformed to unweighted networks by setting a threshold weight  $w^*$  and keeping only connections that are stronger than this weight. For instance in [2] a range of different thresholds is scanned to find the optimal threshold for detecting a global community structure in the network. The authors mention that changing the threshold is like changing the resolution at which we inspect the network's structure.

In this paper we discuss a recent technique from the field of computational topology called *persistent homology* that studies all these different levels of resolution *at once*. Instead of finding the optimal threshold weight, which is often only optimal for a specific property, the framework of persistent homology records structural properties and their changes for a whole range of thresholds.

Persistent homology was not developed with networks in mind, but can be applied in this setting very naturally. For instance, it was previously used to compare normal and abnormal brain networks [3–5]. However, in this work only the zeroth Betti numbers were used. To be able to distinguish two types of abnormal brain networks from normal brain networks the authors needed to include geometrical information by constructing the single linkage dendrograms. Using the Gromov-Hausdorff distance between dendrograms resulted in perfect clustering accuracy. We use the same network filtration as Lee et al. but include the second and first Betti numbers as well as the zeroth Betti numbers.

054  
055  
056  
057  
058  
059  
060  
061  
062  
063  
064  
065  
066  
067  
068  
069  
070  
071  
072  
073  
074  
075  
076  
077  
078  
079  
080  
081  
082  
083  
084  
085  
086  
087  
088  
089  
090  
091  
092  
093  
094  
095  
096  
097  
098  
099  
100  
101  
102  
103  
104  
105  
106  
107

In another paper [6] persistent homology was applied to random, exponential and scale-free networks. There the networks were unweighted and the filtration used is the filtration of  $i$ -skeletons. This leads to a different type of barcode, in particular as the  $j$ -th homology group is zero for all  $i$ -skeletons with  $i < j$  and only depends on the  $j$  and  $j + 1$ -skeleton of a complex, all intervals in the barcode should either persist for just one step in the filtration or forever.

There are already many invariants in use to study the topology of networks. Examples include average path length, small world property, scale-free degree distribution and clustering coefficients. However we think that the robustness and theoretical grounding of persistent homology can give us new insights into the structure of networks.

## 2 Persistent homology of weighted networks

In this section we will introduce concepts from computational topology in the setting of networks. For a more elaborate introduction to persistent homology we refer to [7, 8].

### 2.1 Persistent homology

Persistent homology computes the topological features of a *filtration of a space*. A filtration of a space can be thought of as the evolution of a space or a growing sequence of spaces. More formally a filtration of a space  $X$  is a nested sequence of subspaces beginning with the empty set and ending with  $X$ .

$$\emptyset = X_0 \subseteq X_1 \subseteq \dots \subseteq X_n = X$$

See Figure 1(a) for an illustration of a filtration, where  $X$  is a triangle. Persistent homology computes the classical homology groups of spaces in such a filtration. In this paper we always use homology with  $\mathbb{Z}_2$  coefficients. We write  $H_i(X)$  for the  $i$ -th homology group of  $X$ .<sup>1</sup> The homology groups with coefficients in  $\mathbb{Z}_2$  will always be of the form  $H_i(X) \simeq \mathbb{Z}_2^{\beta_i}$  where  $\beta_i$  is the  $i$ -th Betti number of  $X$ . We are mainly interested in computing these Betti numbers.

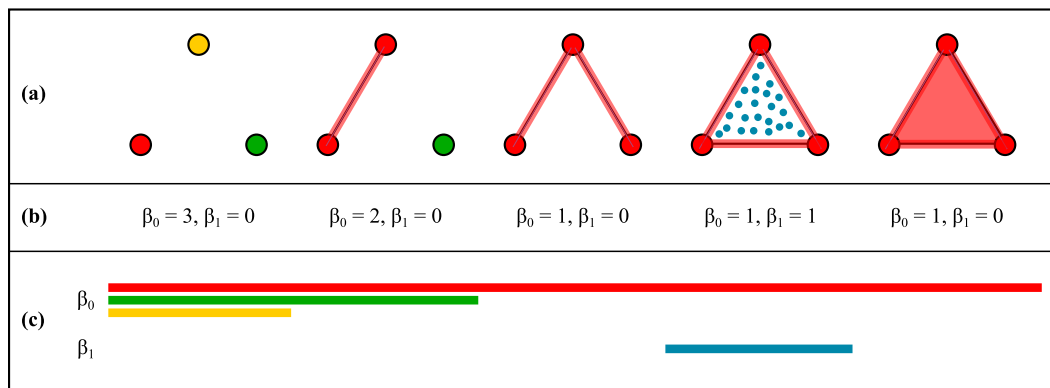


Figure 1: A filtration of a triangle (a). We start with three connected components. The yellow and the green component die in step two and three, but the red component persists the whole filtration. In the fourth step a loop is born, which dies in the final step of the filtration. The zeroth Betti number equals the number of connected components. The first Betti number equals the number of loops (b). We use a barcode to visualise the birth and death of the Betti numbers (c).

Using the inclusion maps  $X_j \rightarrow X_{j+1}$  we can identify copies of  $\mathbb{Z}_2$  in the homology groups  $H_i(X_j)$  and  $H_i(X_{j+1})$  of a filtration. This way we can record when a new copy is *born*, an existing copy *persists* or *dies*. The births and deaths correspond to changes in the topology of the filtration. These changes can be depicted as a barcode [8, 9], where the intervals  $[b_k, d_k]$  correspond to filtration values of the birth and death of an element in the  $i$ -th homology group. The longer a topological feature is present in the filtration, the longer we say it persists. See Figure 1(c).

<sup>1</sup>We are being sloppy with our notation here for increased readability, but should in fact write  $H_i(X; \mathbb{Z}_2)$ .

108 Here, we will restrict our attention to the zero, one and two dimensional homology of spaces. This  
 109 will reduce our computations significantly, since we do not need to include parts of our space that  
 110 are higher dimensional than two-dimensional. We will make this statement more precise in the  
 111 following section.

112 It is well known that  $\beta_0$  equals the number of connected components of a space [10].  $\beta_1$  and  
 113  $\beta_2$  roughly count the number of *loops* and *voids* in a space. We will restrict our results to these  
 114 dimensions, but there are Betti numbers for all positive  $n \in \mathbb{N}$ , corresponding to higher dimensional  
 115 holes in a space. However for finite spaces most of these will be zero since homology groups are  
 116 zero in dimensions larger than the dimension of the space itself.

## 118 2.2 Weighted network

120 A weighted graph is a graph  $G = (V, E)$  together with a weight function  $w : E \rightarrow \mathbb{R}$ . As mentioned  
 121 in the introduction, a weighted graph can be converted to an unweighted graph by keeping only the  
 122 edges stronger than a certain threshold weight  $w^*$ . For a weighted graph  $G$  we will denote this  
 123 threshold subgraph by  $G(w^*)$ . In every threshold subgraph all of the vertices of  $G$  are present.

124 Note that for two different thresholds  $w_i^* > w_j^*$ , we obtain an inclusion  $G(w_i^*) \subseteq G(w_j^*)$ . All edges  
 125 that are present in  $G(w_i^*)$  have weight larger than  $w_i^*$ , so larger than  $w_j^*$ , and thus they are included  
 126 in  $G(w_j^*)$ . For a sequence of weights  $w_0 > w_1 > \dots > w_k$  we obtain a series of graphs and  
 127 inclusions as follows.

$$128 \quad \emptyset \subseteq G(w_0) \subseteq G(w_1) \subseteq \dots \subseteq G(w_k) \subseteq G$$

130 Such a sequence of graph inclusions is called a *graph filtration*.

132 Since a graph can be equipped with a topology to turn it into a one-dimensional space, we can di-  
 133 rectly apply persistent homology to a graph filtration. We will then obtain non-trivial Betti numbers  
 134 in dimension zero and one only.

135 We can encode more of the topological information of the graph into a higher dimensional space; a  
 136 *simplicial complex*. There are many different ways to construct a filtration of simplicial complexes  
 137 from a graph filtration. A common choice is the *clique complex*<sup>2</sup> since it reduces computational  
 138 efforts. [8, 11].

139 We obtain the clique complex of a graph by “filling in” all cliques, that is all complete subgraphs. A  
 140 3-clique will turn into a filled triangle and a 4-clique into a solid tetrahedron and similarly for higher  
 141 dimensional cliques. A nice property of the clique complex is that cliques correspond to highly  
 142 connected groups of nodes that may represent communities [2]. When computing the first Betti  
 143 numbers of such a clique complex we count the number of loops in the complex. In the original  
 144 graph a triangle is a loop and increases the first Betti number by one. In the clique complex all  
 145 triangles are filled and the loop is no longer there, see Figure 1(a). This means that all loops that we  
 146 detect in the clique complex have four or more vertices. The simplest possible loop is formed by  
 147 four vertices connected as a square with no diagonal connections.

148 A vertex is also known as a 0-simplex, an edge as a 1-simplex, a triangle as a 2-simplex and a  
 149 tetrahedron as a 3-simplex. A *face* of a simplex  $\sigma$  is a subsimplex of  $\sigma$ . For instance a triangle has  
 150 six faces, the three edges and three points in its boundary. A simplicial complex is a set of simplices  
 151 such that any face of a simplex is also in the simplicial complex and such that the intersection of any  
 152 two simplices is a face of both.

153 Let  $K$  be the clique complex of a graph  $G$ . The 0-skeleton of  $K$  is the simplicial complex consisting  
 154 of just the vertices of  $G$ . The 1-skeleton of  $K$  is the set of all vertices and edges of  $G$ , i.e. the graph  
 155 itself. The 2-skeleton of  $K$  is the set of all vertices, edges and triangles. In general the  $i$ -skeleton of a  
 156 simplicial complex  $K$  is the subcomplex consisting of all  $j$ -simplices with  $j \leq i$ . We denote the  
 157  $i$ -skeleton by  $K^{(i)}$ . Notice that for  $G'$  a subgraph of  $G$ , the  $i$ -skeleton of the clique complex  $K'^{(i)}$  is  
 158 a subcomplex of  $K^{(i)}$ . This means we obtain a filtration of  $K^{(i)}$  from a graph filtration of  $G$ . And  
 159 in particular since all our clique complexes are finite dimensional, we obtain a filtration of  $K$ .

---

160 <sup>2</sup>the clique complex is also known as the Vietoris Rips complex and the flag-complex. We use the term  
 161 clique complex as it has more meaning in terms of social networks.

162  
163  
164  
165  
166  
167  
168  
169  
170  
171  
172  
173  
174  
175  
176  
177  
178  
179  
180  
181  
182  
183  
184  
185  
186  
187  
188  
189  
190  
191  
192  
193  
194  
195  
196  
197  
198  
199  
200  
201  
202  
203  
204  
205  
206  
207  
208  
209  
210  
211  
212  
213  
214  
215

From the definition of homology we know that the  $i$ -th homology groups of a simplicial complex, and thus the  $i$ -th Betti numbers are completely determined by the  $(i + 1)$ -skeleton. In particular this means that to compute the zero dimensional persistent homology of the clique complex of a graph, we only need the original graph filtration. This is not surprising; the graph contains all connectivity information. Filling in triangles can not change the number of connected components. Moreover making use of this fact we can reduce the computational times for computing Betti numbers in dimension one and two, by only constructing the clique complex up to the 3-skeleton.

### 3 Collaboration networks

We have applied persistent homology to four collaboration networks of scientists [12, 13]. All networks are constructed using a collection of papers. The vertices in the network correspond to the authors of the papers. There is a connection between two scientists if they are co-authors on at least one paper. For each paper that the scientists have collaborated on a weight of  $1/(n - 1)$  is added to the edge. Here  $n$  is the number of authors of the paper. Strong connections correspond to people that collaborate often and in small groups.

Using the above construction we obtain a network that has a very different weight distribution from a more traditional social network as described by Granovetter [1]. In the latter one finds communities of strongly connected individuals and weak ties functioning as local bridges between communities.

Instead, in our collaboration network, weak ties are necessarily part of communities. And in fact, the weaker the tie, the larger the community that it is part of. For example, let two scientist be connected by a weak tie with weight 0.125. This implies that they have co-authored a paper with at least seven other authors<sup>3</sup>. Let us for simplicity assume this is the case. This paper with nine authors corresponds to a 9-clique in our network. All edges in this clique have weight larger or equal to 0.125. If we inspect edges with lower weight than 0.125 we find even more co-authors and larger cliques.

#### 3.1 Collaboration network of network scientists

We will use the network scientists data to explore  $\beta_0$  and  $\beta_1$  in detail. We have restricted our persistence computation to the clique complex of the largest connected component of this collaboration network. This component consists of 379 vertices and 914 edges. The weights in this component range from 0.125 to 4.75.

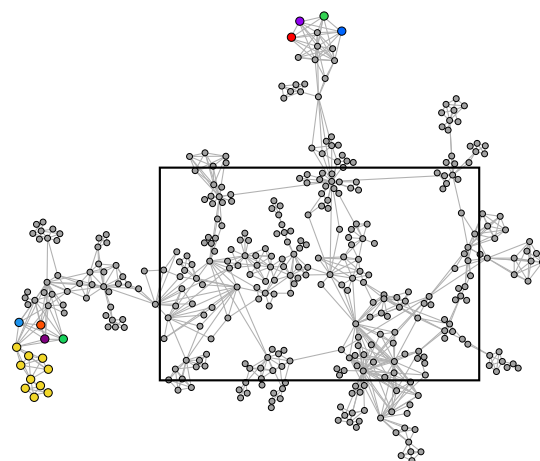


Figure 2: Largest connected component of the network science collaboration network. The enlarged nodes are the nodes that join the largest connected component at the lowest filtration value. Their colours correspond to the component they belonged to before this filtration value is reached.

<sup>3</sup>They could also both have appeared on for instance two papers with 15 authors.

216  
217  
218  
219  
220  
221  
222  
223  
224  
225  
226  
227  
228  
229  
230  
231  
232  
233  
234  
235  
236  
237  
238  
239  
240  
241  
242  
243  
244  
245  
246  
247  
248  
249  
250  
251  
252  
253  
254  
255  
256  
257  
258  
259  
260  
261  
262  
263  
264  
265  
266  
267  
268  
269

Table 1: Collaboration networks

Network	#nodes	#edges	$w^*$	#edges = $w^*$	#edges < $w^*$
Network Science	379	914	0.143	47	10
Condensed Matter	36458	171735	0.034	315	0
High-energy Theory	5835	13815	0.056	171	0
Astrophysics	14845	119652	0.018	357	0

We will first discuss the zeroth Betti numbers of the clique complex filtration. As discussed in the previous section, we may restrict to the 1-skeleton of the complex for this computation, i.e. the graph itself. We start our filtration with  $w^* = 5$ , all vertices of the graph are present but none of the edges are since none of the edges have weight larger than or equal to 5. We immediately find that  $\beta_0 = 379$  since there are 379 connected components, all the individual vertices.

As we lower  $w^*$  in our filtration, more and more edges are added to the graph and  $\beta_0$  will decrease as the graph becomes more connected. Finally  $G(0)$  is connected so we will end with  $\beta_0 = 1$ . In Figure 3(a) we can see how  $\beta_0$  responds to lowering the threshold weight  $w^*$ . We have also plotted the number of edges in the graph and notice that the large decreases in number of connected components correspond to values of  $w^*$  where many edges are added.

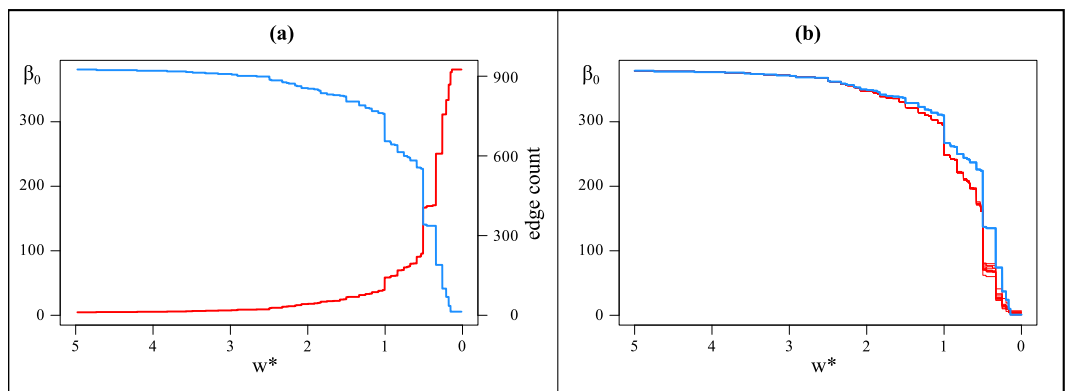
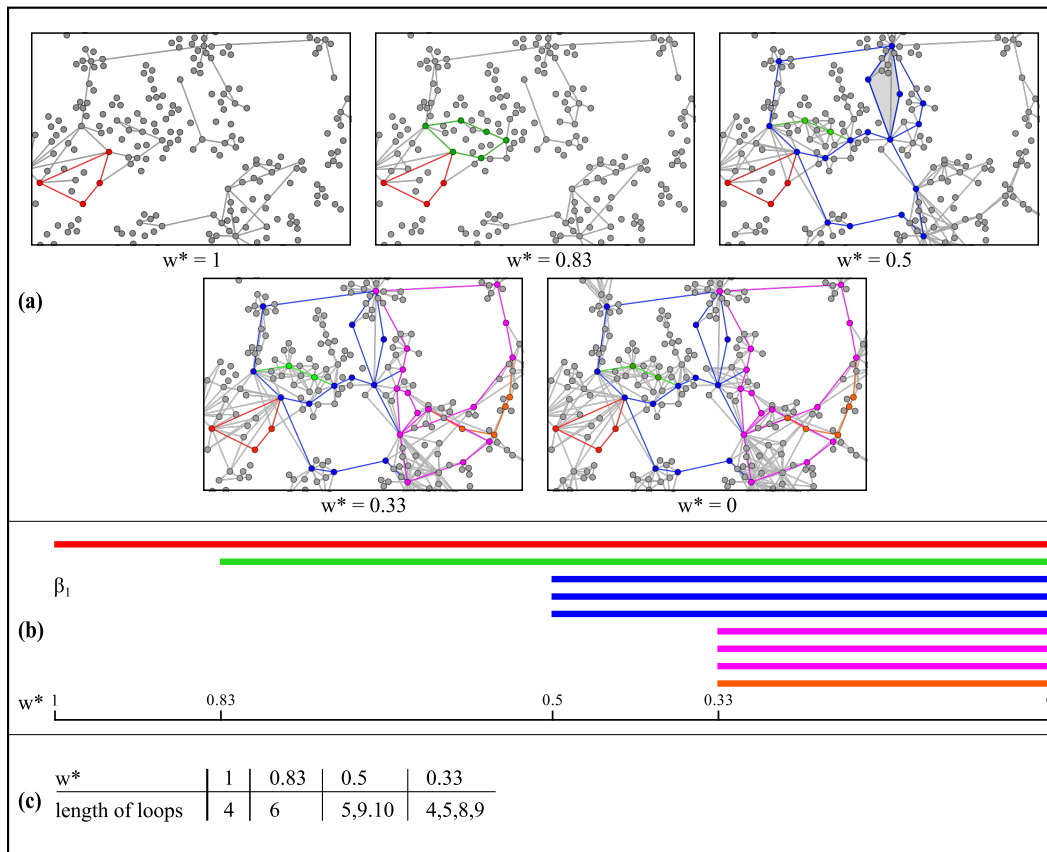


Figure 3: On the left (a) we plot the zeroth Betti number against the threshold  $w^*$  in blue. The total number of edges present at each stage of the filtration is plotted in red. On the right (b) we again plot the zeroth Betti number in blue. There are ten red plots, each corresponding to the sequence of zeroth Betti numbers of a random graphs with the same number of vertices, edges and the same weights.

The network is not connected while  $w^* > 0.143$ . Only after adding the 47 edges with weight equal to 0.143 the network becomes connected, see Table 1. Before adding these edges there are ten components, eight of these consisting of single nodes. We find that these nodes are all part of two 8-cliques, see Figure 2. These authors are only very loosely connected to the rest of the network. We expect that the largest connected component grows rapidly in the filtration and that further lowering the threshold corresponds to adding nodes that are in the periphery of the network. This requires further investigation.

We were curious to see if the zeroth Betti numbers could distinguish this collaboration network from random Erdős-Rényi graphs with the same number of nodes and edges and with the same weights assigned to the edges. We generated 1000 random graphs and used the Bottleneck distance [3, 14] between barcodes to compare the networks. We found that for the random graphs the average pairwise distance was 0.157 (s.d. 0.019) whereas the average distance from the collaboration network to the random graphs was 0.332 (s.d. 0.003). We can definitely use this measure to distinguish the two network topologies. Even though at the start and end of the filtration these networks are very similar we can still detect a structural difference by looking at connected components during the filtration of the networks. In Figure 3(b) we have plotted the zeroth Betti numbers of ten random graphs and the zeroth Betti numbers of the networks scientist collaboration network.

270 Next we inspect the first Betti numbers of the clique complex associated to our network. To do so  
 271 we built the 2-skeleton, which includes all vertices, edges and triangles. Note that a filled triangle  
 272 is added whenever three scientists are pairwise connected. As mentioned in the previous section,  
 273 without filling in these triangles, each triple of pairwise collaborating scientist would be a loop and  
 274 increase the first Betti number by one. However we are interested in the loops in the network on  
 275 a larger scale. In Figure 4 we illustrate the final stages of the graph filtration where the first Betti  
 276 number is non-zero. We show the correspondence between the loops in the complex and the barcode  
 277 we have computed. We find the largest loops for the lowest threshold weights, Figure 3(c). However,  
 278 many of the edges that are part of these loops have high weights.



308 Figure 4: We only show the central part, see Figure 2, of the network of 379 network scientists since all  
 309 loops occur here (a). We find the first relatively small loop between four scientists for appearing for threshold  
 310 weight 1. As we decrease the threshold weight more loops appear. Notice how we have shaded two triangles  
 311 for  $w^* = 0.5$ , this is to indicate that there is no loop there, there are three new blue loops added at this stage.  
 312 We notice that for smaller threshold values we find larger loops. In (b) we show the barcode for the first Betti  
 313 numbers of this filtration. In (c) we enlist the length of the loops that appear at each filtration value.

314 We investigated if the first Betti numbers give us further power to distinguish between the collaboration  
 315 network and the random networks. We found that for random networks we obtain much higher  
 316 first Betti numbers. For 1000 randomly generated networks we found an average of 520.65 (s.d.  
 317 4.39) intervals, while our structured network only has 9 intervals. The reason that this number is  
 318 so much higher for random networks is that there is less clustering and thus fewer triangles that are  
 319 filled in and more loops with more than three edges.

320 Using the first Betti numbers it is enough to only compare the final networks to distinguish between  
 321 random and structured networks. We hope that the persistent homology of the whole filtration will  
 322 be able to detect more subtle structural difference to distinguish networks that are more similar in  
 323 structure. Notice how all of the loops that were born persisted to the end of the filtration. It would  
 have been possible for a loop to die. For instance if the four scientists (A. Vazquez, A. Vespignani,

324  
325  
326  
327  
328  
329  
330  
331  
332  
333  
334  
335  
336  
337  
338  
339  
340  
341  
342  
343  
344  
345  
346  
347  
348  
349  
350  
351  
352  
353  
354  
355  
356  
357  
358  
359  
360  
361  
362  
363  
364  
365  
366  
367  
368  
369  
370  
371  
372  
373  
374  
375  
376  
377

Table 2: Collaboration networks

Network	# intervals $\beta_1$	# intervals $\beta_2$	$\mathbf{p}$	$\alpha$
Condensed Matter	11361	274	0.00026	-0.79
High-energy Theory	1389	2	0.00081	-0.82
Astrophysics	4879	222	0.0011	-0.71

A. Barrat, M. Weigt) appearing in the red loop found at  $w^* = 1$  would have collaborated on a paper, there would be diagonal edges appearing at  $w^* = 0.33$  which would kill the loop.

For this network all higher Betti numbers are trivial.

### 3.2 Physics collaboration networks

In this section we perform analysis on three larger collaboration networks. Again we restrict our attention to the largest connected component of each network. In Table 1 the number of nodes and edges for all of these networks are given. We computed the barcodes for the first three Betti numbers;  $\beta_0, \beta_1, \beta_2$ . We found that  $\beta_0$  stayed high for the largest part of the filtration and then quickly decreased to 1 at the end of the filtration in all three cases. In all cases, the smallest weight was needed to create the connected component, see Table 1. This is slightly different behaviour to the network scientist collaboration network.

We investigated if we can distinguish these collaboration networks from random networks using the persistence barcodes. We notice that all three networks have several intervals corresponding to second Betti numbers.

Let  $G(n, p)$  be an Erdős-Rényi graph with  $p$  the probability of an edge being present, i.e.  $p \sim \frac{2m}{n(n-1)}$ . Erdős and Rényi showed that if  $p \gg \log n/n$  then  $G(n, p)$  is almost always connected [15]. In [16], Kahle shows that there are analogous results for higher dimensional connectivity of the clique complexes of random graphs. In particular, if we define  $\alpha$  by  $p = n^\alpha$ , Kahle shows that the  $k$ -th homology group of a clique complex of a random graph is almost always zero if  $\alpha$  is outside the interval  $(\frac{-1}{k}, \frac{-1}{2k+1})$ . In Table 2 the final values  $\alpha_f$  for the three collaboration networks can be found.

A filtration of a random network corresponds to increasing  $p$  over time, or increasing  $\alpha$  from  $-\infty$  to  $\alpha_f$ . For the clique complex of a random network  $G(n, p)$  we expect the second Betti number to be zero for  $\alpha < -0.5$ . This is the case for all values of  $\alpha$  in our filtration. However we find a large number of intervals for both the condensed matter network and the astrophysics network. This clearly distinguishes these networks from random networks.

Inspection of the zeroth and first Betti numbers is ongoing research.

## 4 Software

We used Gephi [17] for some basic graph manipulations and for graph visualisations. For the persistence computations we used javaPlex [18]. This package was developed to compute the persistent homology of point cloud data. In these computations one starts with a collection of points embedded in Euclidean space, then associates a graph filtration to these points and finally builds a filtration of simplicial complexes of which the persistent homology is computed.

We wrote code in JAVA that imports a weighted edge list and converts it to a graph filtration. Subsequently we used javaPlex to build the clique complex filtration and compute the persistence intervals. The computation of the persistence intervals is the bottleneck in this computation. This took longest for the astrophysics network; 267s (on a MacBook Pro 2.4 GHz Intel Core 2 Duo with 4GB RAM), presumably since it is the densest network. For our current purposes these computation times are sufficient, however if we want to apply the same computations to larger networks we need faster algorithms. This should be possible as described in Chapter 12 of [19]. To generate the random networks with  $n$  vertices and  $m$  edges we wrote code that randomly picks endpoints for  $m$  edges,

378 avoiding double edges and loops. We used the RandomUtility class from javaPlex to pick these  
379 endpoints.  
380

## 381 5 Conclusions 382

383 By applying persistent homology to four collaboration networks of scientists we have shown that  
384 it gives us interesting information about the structure of the networks. We found that due to the  
385 construction of collaboration networks, weak ties form cliques and strong ties act as local bridges  
386 between those cliques. This is contrary to what has been described in other social networks. We  
387 would like to investigate this in greater detail in future work.  
388

389 We were also able to use persistent homology to distinguish these collaboration networks from  
390 random networks. Using the one and two dimensional Betti numbers of the network we did not  
391 need to take the weights into account. We are hoping that using the weights will give us the ability  
392 to distinguish networks that are more similar in structure. This is left as future work.

## 393 Acknowledgments 394

395 Research by both authors was partially supported by the Australian Department of Defence under  
396 Research Agreement 4500743680.  
397

## 400 References 401

- 402 [1] M. Granovetter. The strength of weak ties. *American Journal of Sociology*, 78:1360–80, 1973.  
403 [2] G. Palla, I. Derényi, I. Farkas, and T. Vicsek. Uncovering the overlapping community structure of complex  
404 networks in nature and society. *Nature*, 435:814–818, 2005.  
405 [3] H. Lee, H. Kang, M. Chung, B. Kim, and D. Lee. Persistent brain network homology from the perspective  
406 of dendrogram. *IEEE Transactions on Medical Imaging*, 2012. To appear, available online at [http://ieeexplore.ieee.org/xpls/abs\\_all.jsp?arnumber=6307875](http://ieeexplore.ieee.org/xpls/abs_all.jsp?arnumber=6307875).  
407 [4] H. Lee, M.K. Chung, H. Kang, B.N. Kim, and D.S. Lee. Discriminative persistent homology of brain  
408 networks. In *Biomedical Imaging: From Nano to Macro, 2011 IEEE International Symposium on*, pp.  
409 841–844, 2011.  
410 [5] H. Lee, M. Chung, H. Kang, B. Kim, and D. Lee. Computing the shape of brain networks using graph fil-  
411 tration and Gromov-Hausdorff metric. In *Medical Image Computing and Computer Assisted Intervention*  
412 *(MICCAI), 14th International Conference on*, pp. 289–296, 2011.  
413 [6] D. Horak, S. Maletić, and M. Rajković. Persistent homology of complex networks. *Journal of Statistical*  
414 *Mechanics: Theory and Experiment*, 03:P03034, 2009.  
415 [7] H. Edelsbrunner and J. L. Harer. Persistent homology - a survey. In *Surveys on Discrete and Computa-*  
416 *tional Geometry. Twenty Years Later*, pp. 257–282. American Mathematical Society, 2008.  
417 [8] G. Carlsson. Topology and data. *Bulletin of the American Mathematical Society*, 46(2):255–306, 2009.  
418 [9] R. Ghrist. Barcodes: The persistent topology of data. *Bulletin American Mathematical Society*, 45(1):61–  
419 75, 2008.  
420 [10] A. Hatcher. *Algebraic Topology*. Cambridge University Press, New York, NY, 2002.  
421 [11] A. J. Zomorodian. Fast construction of the Vietoris-Rips complex. *Computers & Graphics*, 34(3):263–  
422 271, 2010.  
423 [12] M.E.J. Newman. The structure of scientific collaboration networks. *Proceedings of the National Academy*  
424 *of Sciences*, 98(2):404–409, 2001.  
425 [13] M.E.J. Newman. Finding community structure in networks using the eigenvectors of matrices. *Physical*  
426 *Review E*, 74(3):036104, 2006.  
427 [14] D. Cohen-Steiner, H. Edelsbrunner, and J. Harer. Stability of persistence diagrams. *Discrete & Compu-*  
428 *tational Geometry*, 37(1):103–120, 2007.  
429 [15] P. Erdős and A. Rényi. On random graphs i. *Publ. Math. Debrecen*, 6:290–297, 1959.  
430 [16] M. Kahle. Topology of random clique complexes. *Discrete Mathematics*, 309(6):1658–1671, 2009.  
431



432  
433  
434  
435  
436  
437  
438  
439  
440  
441  
442  
443  
444  
445  
446  
447  
448  
449  
450  
451  
452  
453  
454  
455  
456  
457  
458  
459  
460  
461  
462  
463  
464  
465  
466  
467  
468  
469  
470  
471  
472  
473  
474  
475  
476  
477  
478  
479  
480  
481  
482  
483  
484  
485

[17] Mathieu Bastian, Sebastien Heymann, and Mathieu Jacomy. Gephi: An open source software for exploring and manipulating networks. Software available at <http://gephi.org>, 2009.

[18] Andrew Tausz, Mikael Vejdemo-Johansson, and Henry Adams. Javaplex: A research software package for persistent (co)homology. Software available at <http://code.google.com/javaplex>, 2011.

[19] A. J. Zomorodian. *Topology for Computing*. Cambridge University Press, England, 2005.